

Impurity scattering in the bulk of topological insulators

Cheung Chan and Tai-Kai Ng

Department of Physics, The Hong Kong University of Science and Technology, Clear Water Bay, Hong Kong

We study in this paper time-reversal δ -impurity scattering effects in the bulk of topological insulators (TI) in two and three dimensions. Specifically we consider how impurity scattering strength is affected by the bulk band structure of topological insulators. An interesting band inversion effect associated with the change of the system from ordinary to topological insulator is pointed out. Experimental consequences of our findings are discussed.

PACS numbers: 71.23.An, 73.20.Hb, 61.72.J-

A. Introduction

Topological insulators (TI) are insulators characterized by a \mathbb{Z}_2 topological number of the bulk band structure, and realize a new topological quantum state protected by time-reversal symmetry^{1,2}. Theoretically, TI are insulating in the bulk but possess gapless boundary states of helical Dirac fermions that give rise to interesting transport properties not realized in ordinary insulators (OI). Novel excitations like Majorana zero modes³ have been proposed to exist in this class of materials and applications of the materials in spintronics have also been discussed⁴.

Towards the applications of TI, a better understanding of the overall properties of the materials beyond their topological surface excitations is needed. For example, to utilize exotic boundary states of TI one needs to ensure a sufficient insulating bulk resistivity, which is a challenge at present due to the presence of bulk conductivity⁵⁻¹⁰ largely arising from the presence of impurities and defects in the materials¹¹. If the defects are external, which is the case for doped materials, one way to attain high bulk resistivity is to synthesize the materials with delicate balance between donors and acceptors^{12,13}. On the other hand, we also want to understand how defects can affect the bulk conductivity through impurity induced in-gap bound states that lead to impurity band and effective narrowing of band gap.

It was pointed out in Ref. 3 that point-like defects in TI do not give rise to topological protected zero-energy states. However, in-gap bound states can still be induced by (isolated) impurities¹⁴⁻¹⁶ through conventional mechanism. For example, depletion of wavefunction at the defect results in-gap bound states if one imagines that the impurity is formed by bending and shrinking the edge into a localized defect¹⁴. However, unlike the (real) edge states, these localized bound states are finite energy modes because they suffer from symmetry allowed (self) interactions. In this paper we consider isolated time-reversal impurities described by δ -function potentials, and study how impurity scattering can depend on the special band structure of TI's. We shall show that impurity scattering can be enhanced in the bulk TI compared with OI due to particular band structure associated with the materials. A criteria to search for materials with suppressed impurity scattering effect is given. An inter-

esting sign-inversion effect in impurity scattering associated with the band inversion in TI-OI transition is also pointed out. Experimental implications of these effects are discussed.

B. Formulation

We adopt the modified Dirac Hamiltonian in either two or three dimensions (2D/3D) as effective models for the topological insulator¹⁴⁻¹⁷, i.e.,

$$H = \sum_{\mathbf{k}, s} \psi_{\mathbf{k}s}^\dagger h_{2(3)D}(\mathbf{k}, s) \psi_{\mathbf{k}s} \quad (1)$$

where $\psi_{\mathbf{k}s}^\dagger (\psi_{\mathbf{k}s})$ are 2-component Dirac fields with momentum and spin indices \mathbf{k} and $s = \uparrow, \downarrow$, respectively and

$$h_{2D}(\mathbf{k}, s) = k_x \sigma^y + k_y \sigma^x s^z + m_k \sigma^z, \quad (2)$$

for 2D topological insulators where σ 's and s 's are Pauli matrices, and $m_k = m - Bk^2$. $\sigma^z = +1(-1)$ describes two contributing atomic orbitals to the topological insulator. For example, they represent s and p states for HgTe/CdTe system. The model can also be generalized to describe 3D topological insulators with a similar effective Hamiltonian $h_{3D}(\mathbf{k}, s)$ with $m_k = m - \sum_i B_i k_i^2$ where $i = x, y, z$ and B_i 's are parameters of the same sign. We shall for simplicity consider $B_x = B_y = B \neq B_z$, corresponding to a common type of topological insulators in 3D with crystal structure $R3m$.

For $mB_i < 0$, the bands are ordered conventionally throughout the Brillouin zone and the system is a ordinary (topologically trivial) insulator. The bands near $\mathbf{k} = 0$ are inverted due to strong spin-orbit coupling for $mB_i > 0$ and the system becomes a topological insulator. The energy eigenvalues of the bulk Hamiltonians are given by $\omega_k = \pm \sqrt{k^2 + (m - \sum B_i k_i^2)^2}$ and are doubly degenerate (Kramers degeneracy). The time reversal operator is given by $\hat{T} = is^y \hat{K}$ with $\hat{T}^2 = -1$, where \hat{K} is the complex conjugate operator.

In real materials there are other electronic bands and impurity scatterings exist in general between the Dirac bands and the other bands. To capture these effects we consider also inter-band scattering between the Dirac

bands with a model quadratic band described by

$$H_q = \sum_{\mathbf{k}s} \left(\frac{k^2}{2M} + \mu \right) c_{\mathbf{k}s}^\dagger c_{\mathbf{k}s}, \quad (3)$$

where M and μ are chosen to have the same sign so that the quadratic band does not cross the Fermi level and the system remains a bulk insulator. $M, \mu > 0$ (< 0) refers to a conduction (valence) band in this notation.

We shall describe the impurity scattering by a single s -wave delta function potential sitting at the origin in this paper. In the four-band modified Dirac model we adopt here, the impurity scattering term within the topological bands can be written in orbital basis¹⁸ as

$$H_{I1} = \hat{u} \delta(\vec{x}), \quad (4)$$

where \hat{u} is a 4×4 matrix. For time reversal impurities \hat{u} should be Hermitian and time reversal symmetric, i.e. $\hat{T} \hat{u} \hat{T}^{-1} = \hat{u}$. There are six bases for \hat{u} , denoted as $u^{(i=0, \dots, 5)} = (I, \sigma^x, \sigma^z, \sigma^y s^x, \sigma^y s^y, \sigma^y s^z)$.

To describe scattering between the topological and quadratic bands, we consider

$$H_{I2} = \sum_{\sigma, s} v_\sigma (\Psi_s^\dagger(0) \psi_{\sigma s}(0) + \psi_{\sigma s}(0)^\dagger \Psi_s(0)), \quad (5)$$

where $\sigma = \pm 1$ and $s = \uparrow, \downarrow$. $\Psi_s(x)$ is the Fourier transform of $c_{\mathbf{k}s}$. We include only spin-independent scattering in writing down H_{I2} .

The effect of impurity scattering is described by the T -matrix defined by

$$\hat{T}(\omega) = \left(\mathbb{I} - \hat{U} \hat{G}_0(\omega) \right)^{-1} \hat{U}, \quad (6a)$$

for the s -wave delta function potential, where \hat{U} is the impurity scattering matrix and $\hat{G}_0(\omega) = \sum_{\mathbf{k}} \hat{G}_0(\mathbf{k}, \omega)$ is the corresponding on-site matrix Green's function. In particular, the existence of impurity bound state is determined by the eigenvalue equation^{19,20}

$$\det \left[\mathbb{I} - \hat{G}_0(\omega) \hat{U} \right] = 0. \quad (6b)$$

For the modified Dirac model, the on-site matrix Green's function in the basis $((1, 1), (-1, 1), (1, -1), (-1, -1))$ (w.r.t. (σ^z, s^z)) is given by

$$\hat{G}_0(\omega) = \begin{bmatrix} g^+(\omega) & & & \\ & g^-(\omega) & & \\ & & g^+(\omega) & \\ & & & g^-(\omega) \end{bmatrix}, \quad (7)$$

where

$$g^\pm(\omega) = - \int d\Omega_D \int_0^\Lambda k^{D-1} dk \frac{\omega \pm m_k}{k^2 + m_k^2 - \omega^2}, \quad (8)$$

where Ω_D is the solid angle in dimension $D = 2, 3$. Λ is a high energy cutoff above which the effective Dirac model

(2) is inadequate in describing the band-structure. Notice that the on-site Green's function matrix \hat{G}_0 involved in Eq. (6b) is diagonal. This is a special feature of the delta-function impurity potential and would be absent if the impurity potential includes higher angular momentum components.

C. $g^\pm(\omega)$ around band-edge and enhanced impurity scattering

Without loss of generality, we shall assume $B > 0$ in the following. We note that in the limit of weak impurity scattering, impurity-induced in-gap bound states can exist only if $g^\pm(\omega)$ diverges near the band edge. In usual (2D) semi-conductors the divergence in $g^\pm(\omega)$ is originated from the band extremum associated with a quadratic band structure. In TI's, the band structure is more complicated and the band extremum may locate at a line of \vec{k} values leading to stronger divergence behavior in $g^\pm(\omega)$. This phenomenon may arise in both 2D and 3D TI's and will lead to enhanced impurity scattering compared with usual semiconductors. First we consider 2D.

1. $2mB < 1$

The integral (8) for $g^\pm(\omega)$ can be evaluated exactly in 2D. For $2mB < 1$ the band minimum is located at $k = 0$ with band gap $|m|$ as in usual semi-conductors. It is straightforward to show that in this case

$$g^\pm(\omega) \Big|_{|\omega| \rightarrow |m|^-} \rightarrow -\pi (\omega \pm m) \ln \left(1 + \frac{\delta^2}{m^2 - \omega^2} \right), \quad (9)$$

where $\delta \sim \min(\Lambda, \sqrt{|m/B|})$ is the momentum cutoff below which we may approximate $m_k \sim m$. We note that a logarithmic divergence appears in $g^\pm(\omega)$ near the band edge when $|\omega| \rightarrow m^-$. Similar logarithmic divergence occurs for quadratic bands with Green's function given by

$$g_0^q(\omega) = -2\pi M \ln \left(1 + \frac{\Lambda^2}{2M(\mu - \omega)} \right). \quad (10)$$

The logarithmic divergence arises from the quadratic dispersion of electron dispersion near the band edge and is responsible for appearance of impurity bound state for arbitrarily weak attractive scattering potential in 2D. Taking $B > 0$, we find that $g^{+(-)}(\omega)$ has logarithmic divergence at $\omega \rightarrow +(-)|m|$ to $-(+)\infty$ for topological insulators (TI) ($m > 0$) and has logarithmic divergence at $\omega \rightarrow -(+)|m|$ to $+(-)\infty$ for ordinary insulators (OI) ($m < 0$), implying that the role of $g^{+(-)}(\omega)$ is inverted when the system changes from OI to TI. Microscopically, a system changes from OI to TI when there is an orbital

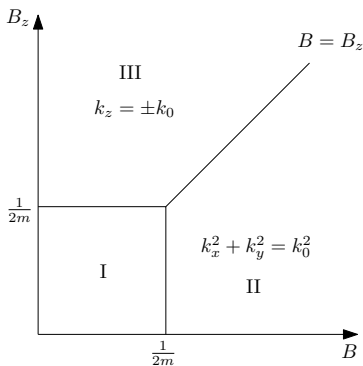


FIG. 1. Parameter range for band extrema k_0 .

inversion ($2m =$ difference in energy between the two orbitals forming the inverted bands) and the inversion in the role of $g^\pm(\omega)$ is a direct consequence of this orbital inversion. In other words, there is a direct correspondence between $g_{\text{TI}}^\pm(\omega) \leftrightarrow g_{\text{OI}}^\mp(\omega)$ with the same band gap $|m|$.

2. $2mB > 1$

In this case, the band extremum occurs at a line of momentum \vec{k} with $|\vec{k}| = k_0$. The corresponding bandgap is given by $\Delta = \frac{\sqrt{4mB-1}}{2|B|}$. Evaluating the integral, we find

$$g^\pm(\omega)|_{|\omega| \rightarrow \Delta^-} \rightarrow -\frac{\pi^2}{\sqrt{2|B|}} \frac{\omega \pm \frac{1}{2B}}{\sqrt{\Delta^2 - \omega^2}} + \text{const.} \quad (11)$$

We see that $g^\pm(\omega)$ has a stronger (inverse square-root) divergence at the gap edge compared with the case $2mB < 1$. This is a result of “dimension reduction” in the integral when the band-minimum occurs at a ring of momentum \vec{k} with $|\vec{k}| = k_0$. We notice that $g^+(\omega)$ diverges to $-(+)\infty$ at $\omega \rightarrow +(-)\Delta$, with a weaker divergence (weighting factor) at $\omega \rightarrow -\Delta$. A similar situation occurs for $g^-(\omega)$ which diverges to $+(-)\infty$ at $\omega \rightarrow -(+)\Delta$, with a weaker divergence at $\omega \rightarrow \Delta$. The appearance of divergences at both $\omega = \pm\Delta$ is possible because of hybridization between the two atomic orbitals. We note that similar double-divergent behavior cannot occur for ordinary insulators which exist only at $mB < 0$.

3. 3D case

We can study $g^\pm(\omega)$ for 3D TI’s in a similar way. Using the Hamiltonian $h_{3D}(\vec{k}, s)$ with $B_x = B_y = B \neq B_z$ we find that the divergent behavior of $g^\pm(\omega)$ can be classified in three different regions as shown in Fig. 1. Region I is defined by $2m(B_z, B) < 1$ with band extremum occurring at $\vec{k} = 0$. Region II is defined by $B > \max(\frac{1}{2m}, B_z)$ with band extremum occurring at

a ring of \vec{k} values, $\vec{k} = (k_x, k_y, 0)$ with $k_x^2 + k_y^2 = k_0^2$ where $k_0 = \frac{1}{B}\sqrt{mB - \frac{1}{2}}$. Region III is defined by $B_z > \max(\frac{1}{2m}, B)$ with band extrema occurring at $\vec{k} = (0, 0, \pm k_0)$ where $k_0 = \frac{1}{B_z}\sqrt{mB_z - \frac{1}{2}}$.

The corresponding Green’s functions are given by

$$\begin{aligned} \frac{g_{\text{I}}^\pm(\omega)}{-4\pi} &\sim \int_0^\delta k^2 dk \frac{\omega \pm m}{k^2 + m^2 - \omega^2} \\ &= (\omega \pm m) \left[\delta - \sqrt{m^2 - \omega^2} \tan^{-1} \left(\frac{\delta}{\sqrt{m^2 - \omega^2}} \right) \right] \\ &\sim \text{const. as } |\omega| \rightarrow |m|^- \end{aligned} \quad (12a)$$

$$\begin{aligned} \frac{g_{\text{II}}^\pm(\omega)}{-2\pi} &\sim \int_{k_0 - \frac{\delta}{2}}^{k_0 + \frac{\delta}{2}} dk \int_0^{\delta_z} dk_z \frac{k_0 (\omega \pm (m - Bk_0^2))}{k^2 + k_z^2 + m_k^2 - \omega^2} \\ &\sim \frac{\omega \pm \frac{1}{2B}}{\sqrt{B(B - B_z)}} \log \left(\frac{1}{\sqrt{\Delta^2 - \omega^2}} \right) \text{ as } |\omega| \rightarrow \Delta^- \end{aligned} \quad (12b)$$

$$\begin{aligned} \frac{g_{\text{III}}^\pm(\omega)}{-2\pi} &\sim \sum_{\gamma=\pm} \int_0^\delta dk \int_{\gamma k_0 - \frac{\delta_z}{2}}^{\gamma k_0 + \frac{\delta_z}{2}} dk_z \frac{k (\omega \pm (m - B_z k_0^2))}{k^2 + k_z^2 + m_k^2 - \omega^2} \\ &\sim \text{const. as } |\omega| \rightarrow \Delta^- \end{aligned} \quad (12c)$$

where $\Delta = \frac{1}{2|B|}\sqrt{4mB - 1}$, where $\bar{B} = B(B_z)$ at region II(III). Here δ, δ_z are momentum cutoff as in Eq. (9). We notice that logarithmic divergence in $g^\pm(\omega \rightarrow \pm\Delta)$ is found for TI in region II which is absent in usual semiconductors which exist only at $mB < 0$. The sign-inversion effect in g_{I}^\pm is also clear although there is no divergence compared with its 2D counterpart.

4. enhanced impurity scattering

The divergence behavior of $g^\pm(\omega)$ has strong implications on impurity scattering behavior described by the T -matrix (6a) where we observe that impurity scattering can be strongly enhanced if $g^\pm(\omega)$ diverges. In particular TI’s with non-diverging $g^\pm(\omega)$ ’s are more robust towards impurity scattering and are better candidates for transport application.

Thus (3D) materials belonging to region I and III are the preferred materials for transport application. For region II, due to the “dimension reduction” effect, divergence appears near the band edges at both $\omega \rightarrow \pm\Delta$ and impurity scattering effects are much enhanced compared with usual semi-conductors. Notice that materials where all B ’s are not equal do not suffer from “dimension reduction” effect and are “preferred” also from the point of view of impurity scattering.

We now apply our analysis to the three TI materials given in Ref. 21, where the low energy spectra around the inverted bands are given by

$$\omega_k = \epsilon_k \pm \sqrt{A_0^2 k_{\parallel}^2 + B_0^2 k_z^2 + M_k^2} \quad (13)$$

material	Bi ₂ Se ₃		Bi ₂ Te ₃		Sb ₂ Te ₃	
band	upper	lower	upper	lower	upper	lower
k_0	0\AA^{-1}	0.09\AA^{-1}	0\AA^{-1}	0.04\AA^{-1}	0.11\AA^{-1}	0.08\AA^{-1}
Region	I	II	I	II	III	III

TABLE I. Band extrema k_0 and corresponding types in Fig. 1 of the inverted band for Bi₂Se₃, Bi₂Te₃ and Sb₂Te₃ (Band parameters are coming from Ref. 21).

where $\epsilon_k = C_1 k_z^2 + C_2 k_{\parallel}^2$, $M_k = M_0 + M_1 k_z^2 + M_2 k_{\parallel}^2$ and $k_{\parallel}^2 = k_x^2 + k_y^2$. Here we neglect the higher order term H_3 which is relevant only for large k . Using the fitting parameters given in Ref. 21 we classify both the upper and lower topological bands for the three materials in Table I. We see from Table I that Bi₂Se₃ and Bi₂Te₃ both have type II band structure and Sb₂Te₃ is the preferred material among the three as far as transport application is concerned.

Impurity-induced in-gap bound states

In this section we consider the formation of impurity induced bound states in the bulk where we shall illustrate the existence of an interesting band-inversion effect. First we focus on the intra-Dirac bands scattering. The scattering matrix respecting \mathcal{T} can be written in orbital basis (the same basis as used in writing down Eq. (7)) as

$$\hat{u} = \begin{bmatrix} u_{11} & u_I & 0 & \tilde{u}_I \\ u_I^* & u_{22} & -\tilde{u}_I & 0 \\ 0 & -\tilde{u}_I^* & u_{11} & u_I^* \\ \tilde{u}_I^* & 0 & u_I & u_{22} \end{bmatrix}, \quad (14)$$

where $u_{11,22} \in \mathbb{R}$ and $u_I, \tilde{u}_I \in \mathbb{C}$. To see the qualitative effect of band structure and TI-OI inversion on bound state formation we consider the case of single scattering channels, i.e. when only one of the u 's in Eq. (14) is non-zero. In this case it is straightforward to obtain the following eigenvalue equations

$$(1 - u_{11}g^+(E))^2 = 0 \quad (15a)$$

$$(1 - u_{22}g^-(E))^2 = 0 \quad (15b)$$

$$(1 - |u_I|^2 g^+(E)g^-(E))^2 = 0 \quad (15c)$$

$$(1 - |\tilde{u}_I|^2 g^+(E)g^-(E))^2 = 0 \quad (15d)$$

for each non-zero u 's where E is the bound state energy. We shall analyse in detail the above equations for the case $2mB < 1$ in 2D. The analysis can be easily generalized to the case $2mB > 1$ and to three dimensions as we shall see in the following.

We start with inter-Dirac-band scattering. Since $g^+(E)g^-(E) < 0$ (c.f. Eq. (9)) in the gap region $|E| < |m|$, the scattering matrix T has no divergence and there

$u_{11} \neq 0$ (Eq. (15a))	$u_{11} > 0$	$u_{11} < 0$
$m > 0$	No	Yes
$m < 0$	Yes	No

$u_{22} \neq 0$ (Eq. (15b))	$u_{22} > 0$	$u_{22} < 0$
$m > 0$	Yes	No
$m < 0$	No	Yes

TABLE II. Single channel intra-Dirac bands scattering induces in-gap bound state in the weak scattering limit. m is the ‘‘gap’’ parameter in the modified-Dirac Hamiltonian.

is no bound state induced by inter-Dirac-band scattering. The situation is very different for intra-band scattering where existence of in-gap bound state depends on the sign of $u_{ii}g^{\pm}(E)$, and it is easy to see that a bound state which appears in the conduction/valence band in OI ($m < 0$) state disappears in the corresponding TI ($m > 0$) state and vice versa, where we have again fixed $B > 0$ for brevity. The results of bound state formation is summarized in Table II. The doubly degeneracy of bound state solutions is a result of Kramer's degeneracy coming from time reversal symmetry. The existence of bound states in these cases is a natural result of an attractive (repulsive) impurity in electron (hole) liquid, which is known to induce bound state in two dimensions for arbitrarily weak potential. The sign change in m just reverses the conduction band to valence band or vice versa but the signs of u 's are not reversed, resulting in the appearance/disappearance of impurity bound states when m changes sign.

We next consider impurity-induced inter-band scattering between the Dirac-bands and an extra quadratic band described by Eq. (5). For simplicity we again consider single scattering channel with either $v_{+(-)}$ being non-zero. It is straightforward to obtain the eigenvalue equations

$$(1 - v_+^2 g^+(E)g_0^q(E))^2 = 0 \quad (16a)$$

$$(1 - v_-^2 g^-(E)g_0^q(E))^2 = 0 \quad (16b)$$

where we again notice the Kramer's degeneracy of the solutions. Notice that unlike inter-Dirac-bands scattering where $g^+(\omega)g^-(\omega) < 0$, independent of the sign of m , $g^{\pm}(E)g_0^q(E)$ depends now on the sign of m . The resulting bound state formation possibilities are summarized in Table III where we have considered the quadratic band to be either a conduction or valence band. Notice that the results are independent of the sign of the impurity potential since v_{σ} always enters the eigenvalue equation as v_{σ}^2 . Again if we fix the scattering channel and the quadratic band, we find that the bound state appears/disappears when m changes sign because the sign of $g^{+(-)}(E)$ changes upon orbital inversion. Our analysis can be extended easily to the case $2mB > 1$. There is no band-inversion effect in this case since ordinary insulator exists only for $mB < 0$ and impurity bound state

always exist because of the “double-divergence” behavior in $g^\pm(\omega)$. The situation for 3D TIs are similar. Band inversion effect exist only in Region I and weak impurity bound state always exist in Region II.

$v_+ \neq 0$ (Eq. (16a))	$M, \mu > 0$	$M, \mu < 0$
$m > 0$	Yes	No
$m < 0$	No	Yes

$v_- \neq 0$ (Eq. (16b))	$M, \mu > 0$	$M, \mu < 0$
$m > 0$	No	Yes
$m < 0$	Yes	No

TABLE III. Induced in-gap bound states resulting from weak inter-Dirac-quadratic band scatterings. Quadratic bands are described by $M, \mu > 0$ (conduction) or < 0 (valence), and m is the “gap” parameter of the modified-Dirac equation.

D. Summary

We are now in the position to discuss and summarize our results. We show that impurity scattering effect in TI with band structure parameters in certain region are enhanced compared with usual semi-conductors. As a result impurity bound states can form easily in these TIs, leading to enhanced bulk conductivity and reduced effective band-gap. Impurity scattering effect can be reduced for TIs with band parameters in suitable region (region I and III in Fig. 1 for 3D TIs). Our analysis is applied to three materials Bi_2Se_3 , Bi_2Te_3 and Sb_2Te_3 where we find

that Sb_2Te_3 is the preferred material among the three as far as transport application is concerned. We note that a larger variety of TI materials exist nowadays and our analysis can be applied if their band structure is known.

We also point out another interesting sign-inversion effect associated with band inversion in TI-OI transition. The effect is most pronounced in 2D TI with $2mB < 1$. Experimentally, the TI-OI transition can be controlled by gate voltage in InAs/GaSb quantum well system and the transport measurement can be carried out at various chemical potentials inside the band gap^{22,23}. The band inversion effect can be observed through a change in distribution of impurity bound state energies when the system changes from TI to OI state. The effect is strongest if the impurities coupled preferably to one of the atomic orbitals.

In conclusion, we study the effect of impurity scattering in TIs in this paper. Our work is complimentary to previous works^{14–16} that consider impurity bound state forming from continuous deformation of edge modes. We find that impurity-induced bound state formation depends strongly on the band structure of the TIs and impurity scattering can be suppressed in TIs with band structures in the correct region. Our result provides a guidance for TI material engineering which is useful for search of applicable TIs.

ACKNOWLEDGMENTS

We acknowledge helpful discussion with S. Q. Shen. This work is supported by HKRGC through grant CRF09/HKUST03.

-
- ¹ M. Z. Hasan and C. L. Kane, Rev. Mod. Phys. **82**, 3045 (2010).
² X.-L. Qi and S.-C. Zhang, Rev. Mod. Phys. **83**, 1057 (2011).
³ J. C. Y. Teo and C. L. Kane, Phys. Rev. B **82**, 115120 (2010).
⁴ J. E. Moore, Nature **464**, 194 (2010).
⁵ J. G. Checkelsky, Y. S. Hor, M.-H. Liu, D.-X. Qu, R. J. Cava, and N. P. Ong, Phys. Rev. Lett. **103**, 246601 (2009).
⁶ D.-X. Qu, Y. S. Hor, J. Xiong, R. J. Cava, and N. P. Ong, Science **329**, 821 (2010).
⁷ J. G. Analytis, R. D. McDonald, S. C. Riggs, J.-H. Chu, G. S. Boebinger, and I. R. Fisher, Nat Phys **6**, 960 (2010).
⁸ J. G. Analytis, J.-H. Chu, Y. Chen, F. Corredor, R. D. McDonald, Z. X. Shen, and I. R. Fisher, Phys. Rev. B **81**, 205407 (2010).
⁹ K. Eto, Z. Ren, A. A. Taskin, K. Segawa, and Y. Ando, Phys. Rev. B **81**, 195309 (2010).
¹⁰ N. P. Butch, K. Kirshenbaum, P. Syers, A. B. Sushkov, G. S. Jenkins, H. D. Drew, and J. Paglione, Phys. Rev. B **81**, 241301 (2010).
¹¹ Z. Ren, A. A. Taskin, S. Sasaki, K. Segawa, and Y. Ando, Phys. Rev. B **82**, 241306 (2010).
¹² Z. Ren, A. A. Taskin, S. Sasaki, K. Segawa, and Y. Ando, Phys. Rev. B **84**, 165311 (2011).
¹³ J. Xiong, A. C. Petersen, D. Qu, R. J. Cava, and N. P. Ong, ArXiv e-prints (2011), arXiv:1101.1315 [cond-mat.mes-hall].
¹⁴ W.-Y. Shan, J. Lu, H.-Z. Lu, and S.-Q. Shen, Phys. Rev. B **84**, 035307 (2011).
¹⁵ S.-Q. Shen, W.-Y. Shan, and H.-Z. Lu, ArXiv e-prints (2010), arXiv:1009.5502 [cond-mat.mes-hall].
¹⁶ J. Lu, W.-Y. Shan, H.-Z. Lu, and S.-Q. Shen, New Journal of Physics **13**, 103016 (2011).
¹⁷ L. Fu and C. L. Kane, Phys. Rev. B **76**, 045302 (2007).
¹⁸ V. V. Cheianov and V. I. Fal’ko, Phys. Rev. Lett. **97**, 226801 (2006).
¹⁹ A. V. Balatsky, I. Vekhter, and J.-X. Zhu, Rev. Mod. Phys. **78**, 373 (2006).
²⁰ T. K. Ng and Y. Avishai, Phys. Rev. B **80**, 104504 (2009).
²¹ C.-X. Liu, X.-L. Qi, H. Zhang, X. Dai, Z. Fang, and S.-C. Zhang, Phys. Rev. B **82**, 045122 (2010).
²² I. Knez, R.-R. Du, and G. Sullivan, Phys. Rev. Lett. **107**, 136603 (2011).
²³ I. Knez, R.-R. Du, and G. Sullivan, ArXiv e-prints (2011), arXiv:1106.5819 [cond-mat.mes-hall].